

Crystal structure, synthesis and thermal properties of bis(acetonitrile- κ N)bis(4-benzoylpyridine- κ N)-bis(isothiocyanato- κ N)nickel(II)

Carsten Wellm* and Christian Näther

Institut für Anorganische Chemie, Universität Kiel, Max-Eyth-Strasse 2, 241128 Kiel, Germany. *Correspondence e-mail: cwellm@ac.uni-kiel.de

Received 30 September 2019

Accepted 9 October 2019

Edited by A. J. Lough, University of Toronto, Canada

Keywords: crystal structure; nickel(II) thiocyanate; solvate; discrete complex; hydrogen bonding.

CCDC references: 1958279; 1958279

Supporting information: this article has supporting information at journals.iucr.org/e

In the crystal structure of the title compound, $[\text{Ni}(\text{NCS})_2(\text{CH}_3\text{CN})_2(\text{C}_{12}\text{H}_9\text{NO})_2]$ or $\text{Ni}(\text{NCS})_2(4\text{-benzoylpyridine})_2(\text{acetonitrile})_2$, the Ni^{II} ions are octahedrally coordinated by the N atoms of two thiocyanate anions, two 4-benzoylpyridine ligands and two acetonitrile molecules into discrete complexes that are located on centres of inversion. In the crystal, the discrete complexes are linked by centrosymmetric pairs of weak $\text{C}-\text{H}\cdots\text{S}$ hydrogen bonds into chains. Thermogravimetric measurements prove that, upon heating, the title complex loses the two acetonitrile ligands and transforms into a new crystalline modification of the chain compound $[\text{Ni}(\text{NCS})_2(4\text{-benzoylpyridine})_2]$, which is different from that of the corresponding Co^{II} , Ni^{II} and Cd^{II} coordination polymers reported in the literature. IR spectroscopic investigations indicate the presence of bridging thiocyanate anions but the powder pattern cannot be indexed and, therefore, this structure is unknown.

1. Chemical context

In most cases, the synthesis of new coordination compounds is performed in solution, which in some cases leads to inhomogeneous samples or some, *e.g.* metastable compounds, formed by kinetic control which can easily be overlooked. There are, however, some alternative routes, like synthesis *via* molecular milling, molten flux synthesis, solid-gas reactions or thermal decomposition of suitable precursor compounds (Braga *et al.*, 2005, 2006; Näther *et al.*, 2013; Zurawski *et al.*, 2012; Höller *et al.*, 2008; Den *et al.*, 2019). These methods can have several advantages because, in most cases, they are irreversible, the products are obtained in quantitative yield, no solvent is needed and sometimes metastable isomeric or polymorphic modifications can be obtained. This is especially the case for thiocyanate coordination polymers prepared by thermal decomposition of suitable precursor compounds that consist of complexes in which the anionic ligands are only terminally bonded and additionally coordinated by neutral N-donor co-ligands (Wöhlert *et al.*, 2014; Werner *et al.*, 2015). Upon heating, the co-ligands are stepwise removed, leading to new compounds in which the metal cations are linked by thiocyanate anions into chains or layers (Neumann *et al.*, 2019). In this context, we have reported on coordination polymers based on 4-benzoylpyridine. In $[\text{M}(\text{NCS})_2(4\text{-benzoylpyridine})_2]$ ($M = \text{Co}$ and Ni) prepared in solution, a rare *cis-cis-trans* coordination is observed, in which the thiocyanate N and S atoms are each in *cis* positions, whereas the co-ligand is *trans* (Rams *et al.*, 2017; Jochim *et al.*, 2018). This is in contrast to all other linear chain compounds, in which the coordinating atoms always show an *all-trans* coordination. Surprisingly, this

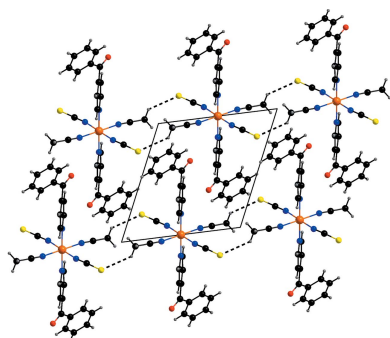


Table 1
Selected geometric parameters (Å, °).

Ni1—Ni1 ⁱ	2.038 (3)	Ni1—N2 ⁱ	2.093 (2)
Ni1—N1	2.038 (3)	Ni1—N11 ⁱ	2.108 (2)
Ni1—N2	2.093 (2)	Ni1—N11	2.108 (2)
N1 ⁱ —Ni1—N1	180.0	N1 ⁱ —Ni1—N11	89.97 (9)
N1 ⁱ —Ni1—N2	91.36 (9)	N1—Ni1—N11	90.03 (9)
N1—Ni1—N2	88.64 (9)	N2—Ni1—N11	89.69 (8)
N1 ⁱ —Ni1—N2 ⁱ	88.64 (9)	N2 ⁱ —Ni1—N11	90.31 (8)
N1—Ni1—N2 ⁱ	91.36 (9)	N11 ⁱ —Ni1—N11	180.0
N2—Ni1—N2 ⁱ	180.0	C1—N1—Ni1	163.8 (2)
N1 ⁱ —Ni1—N11 ⁱ	90.03 (9)	C15—N11—Ni1	121.05 (18)
N1—Ni1—N11 ⁱ	89.97 (9)	C11—N11—Ni1	121.64 (17)
N2—Ni1—N11 ⁱ	90.31 (8)	C2—N2—Ni1	171.5 (2)
N2 ⁱ —Ni1—N11 ⁱ	89.69 (8)		

Symmetry code: (i) $-x + 2, -y + 1, -z + 2$.

coordination is found in $[\text{Cd}(\text{NCS})_2(4\text{-benzoylpyridine})_2]$ (Neumann *et al.*, 2018). Therefore, the question arose if this form can be prepared with Ni by thermal decomposition using a suitable Ni^{II} precursor compound. One discrete complex with methanol has already been reported in the literature, but this compound cannot be prepared pure (Wellm & Näther, 2019a). In the course of this project, we were able to prepare crystals from acetonitrile, which were characterized by single-crystal structure analysis, which proves that the title compound consists of discrete complexes with the composition $\text{Ni}(\text{NCS})_2(4\text{-benzoylpyridine})_2(\text{acetonitrile})_2$. This compound can be prepared pure and is a promising precursor to prepare

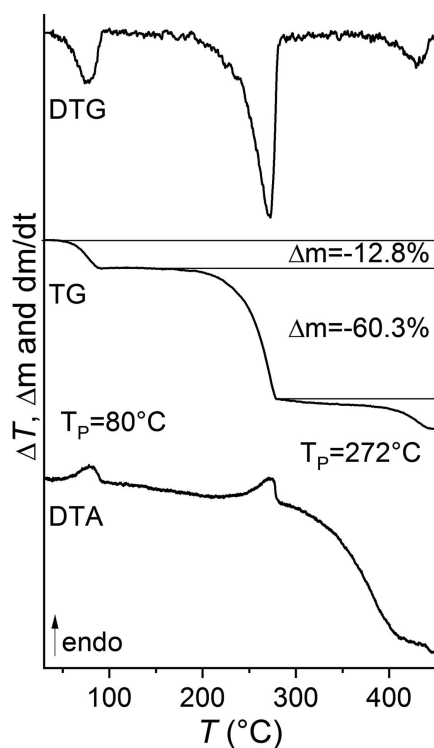


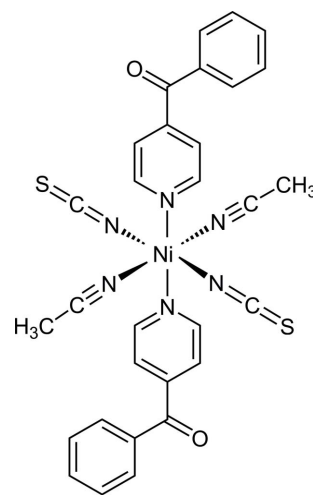
Figure 1
DTG, TG and DTA curve of the title compound with the experimental mass loss in % and the peak temperatures in °C. The calculated mass loss of two MeCN molecules amounts to 13.2% and the loss of two 4-benzoylpyridine ligands corresponds to 58.8%.

Table 2
Hydrogen-bond geometry (Å, °).

$D-H\cdots A$	$D-H$	$H\cdots A$	$D\cdots A$	$D-H\cdots A$
C3—H3B \cdots S1 ⁱⁱ	0.98	2.98	3.662 (3)	127

Symmetry code: (ii) $-x + 2, -y + 2, -z + 2$.

an Ni^{II} compound with bridging thiocyanate anions (Fig. S1 in the supporting information). Measurements using differential thermoanalysis and thermogravimetry (DTA–TG) prove that on heating two mass steps are observed that are accompanied by endothermic events in the DTA curve (Fig. 1). The experimental mass loss of 12.8% in the first step is in reasonable agreement with that calculated for the removal of two acetonitrile molecules of 13.1%, indicating the formation of a compound with the desired composition (Fig. 1). If the X-ray powder diffraction pattern of the residue formed after the first mass loss is compared with that calculated for $[\text{Ni}(\text{NCS})_2(4\text{-benzoylpyridine})_2]$ reported in the literature, it is obvious that a crystalline phase has been formed (Fig. S1 in the supporting information). This new form is also different from $[\text{Cd}(\text{NCS})_2(4\text{-benzoylpyridine})_2]$, indicating that a new isomeric or polymorphic form is obtained. The value of the CN stretching vibration of this form (2113 cm^{-1}) is very different from that of the title compound (2080 cm^{-1}) but comparable to that observed in the known modification of $[\text{Ni}(\text{NCS})_2(4\text{-benzoylpyridine})_2]$ (2121 cm^{-1}) reported in the literature (Jochim *et al.*, 2018), which indicates a similar thiocyanate coordination (Figs. S2, S3 and S4 in the supporting information). However, this powder pattern cannot be indexed and thus the structure of this new form is unknown.



2. Structural commentary

The asymmetric unit of the title compound consists of one Ni^{II} ion that is located on a centre of inversion, as well as one thiocyanate anion, one 4-benzoylpyridine co-ligand and one acetonitrile ligand that occupy general positions (Fig. 2). The Ni^{II} ions are sixfold coordinated by the N atoms of two terminal thiocyanate anions, two 4-benzoylpyridine and two

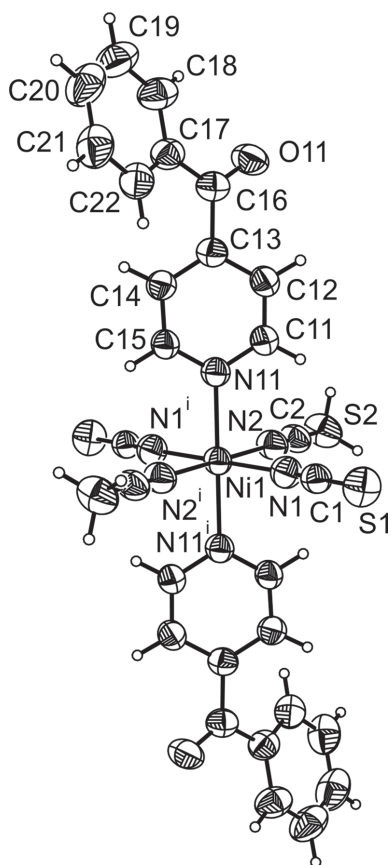


Figure 2
The molecular structure of the title compound with labelling and displacement ellipsoids drawn at the 50% probability level. [Symmetry code: (i) $-x + 2, -y + 1, -z + 2$]

acetonitrile ligands (Fig. 2). The Ni–NCS bond length to the negatively charged anionic ligands of 2.038 (3) Å is shorter than the Ni–N(pyridine) and Ni–NCMe bond lengths of

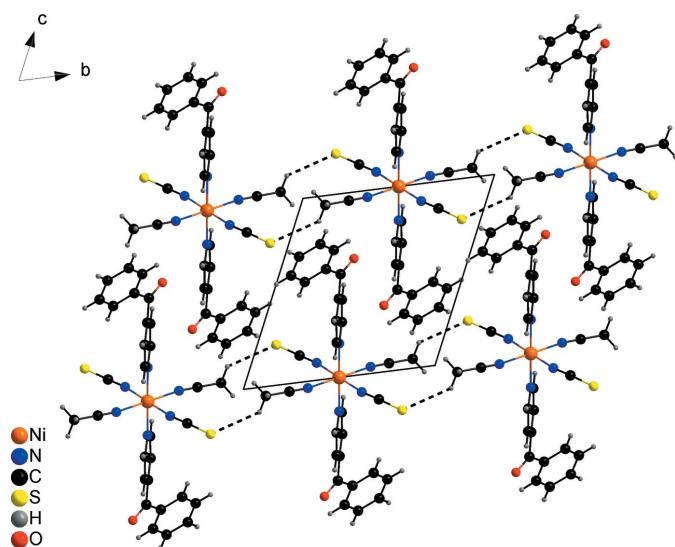


Figure 3
Part of the crystal structure of the title compound, viewed along the crystallographic a axis, and with intermolecular C–H...S hydrogen bonding shown as dashed lines.

2.108 (2) and 2.108 (2) Å, respectively (Table 1). The bond angles deviate only slightly from ideal values, which shows that the octahedra are only slightly distorted (Table 1). This is also obvious from the octahedral angle variance of 0.71 and the quadratic elongation of 1.0006 calculated according to a procedure published by Robinson *et al.* (1971). The dihedral angle between the carbonyl plane (C13/C16/C17/O11) and that of the phenyl (C17–C22) ring is 22.2 (2)°, and that between the planes of the pyridine ring (N11/C11–15) and the carbonyl group (C13/C16/C17/O11) is 33.7 (2)°, which shows that the 4-benzoylpyridine ligand is not coplanar.

3. Supramolecular features

The discrete complexes are arranged into columns that proceed along the crystallographic a axis (Fig. 3). Along the b axis they are linked into chains by centrosymmetric pairs of weak C–H...S hydrogen bonds between the acetonitrile H atoms and the thiocyanate S atoms (Fig. 3 and Table 2).

4. Database survey

There are already some compounds reported in the Cambridge Structural Database (Groom *et al.*, 2016) that consist of transition-metal thiocyanates and 4-benzoylpyridine ligands. These are Zn(NCS)₂(4-benzoylpyridine)₂ with tetrahedrally coordinated Zn^{II} cations (Neumann *et al.*, 2018) and Cu(NCS)₂(4-benzoylpyridine)₂ in which the Cu^{II} cations are square-planar coordinated (Bai *et al.*, 2011). There are also a number of discrete complexes with an octahedral metal coordination and terminal thiocyanate anions (Drew *et al.*, 1985; Soliman *et al.*, 2014; Wellm & Näther, 2018, 2019a,b; Neumann *et al.*, 2018; Suckert *et al.*, 2017). Finally, there are several coordination polymers with the composition [M(NCS)₂(4-benzoylpyridine)₂]_n ($M = \text{Cd}^{\text{II}}, \text{Ni}^{\text{II}}$ and Co^{II}), in which the cations are linked by pairs of μ -1,3-coordinating thiocyanate anions into chains (Neumann *et al.*, 2018; Rams *et al.*, 2017; Jochim *et al.*, 2018).

5. Synthesis and crystallization

Ba(SCN)₂·3H₂O and 4-benzoylpyridine were purchased from Alfa Aesar. Ni(SO₄)·6H₂O was purchased from Merck. All solvents and reactants were used without further purification.

Ni(NCS)₂ was prepared by the reaction of equimolar amounts of Ni(SO₄)·6H₂O and Ba(SCN)₂·3H₂O in water. The resulting white precipitate of BaSO₄ was filtered off, and the solvent was evaporated from the filtrate. The green solid was dried at room temperature.

5.1. Synthesis

Crystals of the title compound suitable for single-crystal X-ray diffraction were obtained by the reaction of Ni(NCS)₂ (26.2 mg, 0.15 mmol) with 4-benzoylpyridine (27.5 mg, 0.15 mmol) in acetonitrile (1.5 ml) for 2 d at 354 K in a closed test tube. A polycrystalline powder was obtained by stirring a

Table 3
Experimental details.

Crystal data	
Chemical formula	[Ni(NCS) ₂ (C ₂ H ₂ N ₂) ₂ (C ₁₂ H ₉ NO) ₂]
<i>M</i> _r	623.38
Crystal system, space group	Triclinic, <i>P</i> $\bar{1}$
Temperature (K)	200
<i>a</i> , <i>b</i> , <i>c</i> (Å)	7.2716 (5), 10.4868 (6), 10.8677 (6)
α , β , γ (°)	65.540 (4), 88.893 (5), 88.378 (5)
<i>V</i> (Å ³)	754.02 (8)
<i>Z</i>	1
Radiation type	Mo <i>K</i> α
μ (mm ⁻¹)	0.82
Crystal size (mm)	0.14 × 0.05 × 0.04
Data collection	
Diffraction	Stoe IPDS2
Absorption correction	Numerical (<i>X-SHAPE</i> and <i>X-RED32</i> ; Stoe & Cie, 2008)
<i>T</i> _{min} , <i>T</i> _{max}	0.837, 0.966
No. of measured, independent and observed [<i>I</i> > 2 σ (<i>I</i>)] reflections	9692, 3283, 2634
<i>R</i> _{int}	0.041
(<i>sin</i> θ / λ) _{max} (Å ⁻¹)	0.639
Refinement	
<i>R</i> [<i>F</i> ² > 2 σ (<i>F</i> ²)], <i>wR</i> (<i>F</i> ²), <i>S</i>	0.046, 0.100, 1.06
No. of reflections	3283
No. of parameters	188
H-atom treatment	H-atom parameters constrained
$\Delta\rho_{\max}$, $\Delta\rho_{\min}$ (e Å ⁻³)	0.28, -0.40

Computer programs: *X-AREA* (Stoe & Cie, 2008), *SHELXS97* (Sheldrick, 2008), *SHELXL2014* (Sheldrick, 2015), *XP* in *SHELXTL* (Sheldrick, 2008) and *DIAMOND* (Brandenburg, 1999) and *pubCIF* (Westrip, 2010).

solution of Ni(NCS)₂ (87.4 mg, 0.5 mmol) and 4-benzoylpyridine (183.2 mg, 1.0 mmol) in MeCN (3 ml) for 4 d.

5.2. Experimental details

Differential thermoanalysis and thermogravimetry (DTA–TG) were performed under a dynamic nitrogen atmosphere in Al₂O₃ crucibles using an STA PT1600 thermobalance from Linseis. The XRPD measurements were performed using a Stoe Transmission Powder Diffraction System (STADI P) with Cu *K* α radiation that was equipped with a linear position-sensitive MYTHEN detector from Stoe & Cie. The IR data were measured using a Bruker Alpha-P ATR–IR spectrometer.

6. Refinement

The C–H hydrogens were positioned with idealized geometry (methyl H atoms allowed to rotate but not to tip) and refined with *U*_{iso}(H) = 1.2*U*_{eq}(C) (1.5 for methyl H atoms) using a riding model. Crystal data, data collection and structure refinement details are summarized in Table 3.

Acknowledgements

This project was supported by the Deutsche Forschungsgemeinschaft and the State of Schleswig-Holstein. We thank

Professor Dr Wolfgang Bensch for access to his experimental facilities.

Funding information

Funding for this research was provided by: Deutsche Forschungsgemeinschaft (grant No. NA 720/5-2).

References

- Bai, Y., Zheng, G.-S., Dang, D.-B., Zheng, Y.-N. & Ma, P.-T. (2011). *Spectrochim. Acta A Mol. Biomol. Spectrosc.* **79**, 1338–1344.
- Braga, D., Curzi, M., Grepioni, F. & Polito, M. (2005). *Chem. Commun.* pp. 2915–2917.
- Braga, D., Giuffreda, S. L., Grepioni, F., Pettersen, A., Maini, L., Curzi, M. & Polito, M. (2006). *Dalton Trans.* pp. 1249–1263.
- Brandenburg, K. (1999). *DIAMOND*. Crystal Impact GbR, Bonn, Germany.
- Den, T., Usov, P. M., Kim, J., Hashizume, D., Ohtsu, H. & Kawano, M. (2019). *Chem. Eur. J.* **25**, 11512–11520.
- Drew, M. G. B., Gray, N. I., Cabral, M. F. & Cabral, J. O. (1985). *Acta Cryst.* **C41**, 1434–1437.
- Groom, C. R., Bruno, I. J., Lightfoot, M. P. & Ward, S. C. (2016). *Acta Cryst.* **B72**, 171–179.
- Höller, C. J. & Müller-Buschbaum, K. (2008). *Inorg. Chem.* **47**, 10141–10149.
- Jochim, A., Rams, M., Neumann, T., Wellm, C., Reinsch, H., Wójtowicz, G. M. & Näther, C. (2018). *Eur. J. Inorg. Chem.* **2018**, 4779–4789.
- Näther, C., Wöhlert, S., Boeckmann, J., Wriedt, M. & Jess, I. (2013). *Z. Anorg. Allg. Chem.* **639**, 2696–2714.
- Neumann, T., Jess, I., dos Santos Cunha, C., Terraschke, H. & Näther, C. (2018). *Inorg. Chim. Acta*, **478**, 15–24.
- Neumann, T., Rams, M., Tomkowicz, Z., Jess, I. & Näther, C. (2019). *Chem. Commun.* **55**, 2652–2655.
- Rams, M., Tomkowicz, Z., Böhme, M., Plass, W., Suckert, S., Werner, J., Jess, I. & Näther, C. (2017). *Phys. Chem. Chem. Phys.* **19**, 3232–3243.
- Robinson, K., Gibbs, G. V. & Ribbe, P. H. (1971). *Science*, **172**, 567–570.
- Sheldrick, G. M. (2008). *Acta Cryst.* **A64**, 112–122.
- Sheldrick, G. M. (2015). *Acta Cryst.* **C71**, 3–8.
- Soliman, S. M., Elzawy, Z. B., Abu-Youssef, M. A. M., Albering, J., Gatterer, K., Öhrström, L. & Kettle, S. F. A. (2014). *Acta Cryst.* **B70**, 115–125.
- Stoe & Cie (2008). *X-AREA*, *X-RED32* and *X-SHAPE*. Stoe & Cie, Darmstadt, Germany.
- Suckert, S., Werner, J., Jess, I. & Näther, C. (2017). *Acta Cryst.* **E73**, 365–368.
- Wellm, C. & Näther, C. (2018). *Acta Cryst.* **E74**, 1899–1902.
- Wellm, C. & Näther, C. (2019a). *Acta Cryst.* **E75**, 299–303.
- Wellm, C. & Näther, C. (2019b). *Acta Cryst.* **E75**, 917–920.
- Werner, J., Runčevski, T., Dinnebier, R., Ebbinghaus, S. G., Suckert, S. & Näther, C. (2015). *Eur. J. Inorg. Chem.* **2015**, 3236–3245.
- Westrip, S. P. (2010). *J. Appl. Cryst.* **43**, 920–925.
- Wöhlert, S., Runčevski, T., Dinnebier, T., Ebbinghaus, S. G. & Näther, C. (2014). *Cryst. Growth Des.* **14**, 1902–1913.
- Zurawski, A., Rybak, J. C., Meyer, L. V., Matthes, P. R., Stepanenko, V., Dannenbauer, N., Würthner, F. & Müller-Buschbaum, K. (2012). *Dalton Trans.* **41**, 4067–4078.

supporting information

Acta Cryst. (2019). E75, 1685-1688 [https://doi.org/10.1107/S2056989019013756]

Crystal structure, synthesis and thermal properties of bis(acetonitrile- κ N)bis(4-benzoylpyridine- κ N)bis(isothiocyanato- κ N)nickel(II)

Carsten Wellm and Christian Näther

Computing details

Data collection: *X-AREA* (Stoe & Cie, 2008); cell refinement: *X-AREA* (Stoe & Cie, 2008); data reduction: *X-AREA* (Stoe & Cie, 2008); program(s) used to solve structure: *SHELXS97* (Sheldrick, 2008); program(s) used to refine structure: *SHELXL2014* (Sheldrick, 2015); molecular graphics: *XP* in *SHELXTL* (Sheldrick, 2008) and *DIAMOND* (Brandenburg, 1999); software used to prepare material for publication: *pubCIF* (Westrip, 2010).

Bis(acetonitrile- κ N)bis(4-benzoylpyridine- κ N)bis(isothiocyanato- κ N)nickel(II)

Crystal data

[Ni(NCS)₂(C₂H₂N₂₁)₂(C₁₂H₉NO)₂]

$M_r = 623.38$

Triclinic, $P\bar{1}$

$a = 7.2716$ (5) Å

$b = 10.4868$ (6) Å

$c = 10.8677$ (6) Å

$\alpha = 65.540$ (4)°

$\beta = 88.893$ (5)°

$\gamma = 88.378$ (5)°

$V = 754.02$ (8) Å³

$Z = 1$

$F(000) = 322$

$D_x = 1.373$ Mg m⁻³

Mo $K\alpha$ radiation, $\lambda = 0.71073$ Å

Cell parameters from 9692 reflections

$\theta = 2.1$ – 25.2 °

$\mu = 0.82$ mm⁻¹

$T = 200$ K

Needle, blue

$0.14 \times 0.05 \times 0.04$ mm

Data collection

Stoe IPDS-2
diffractometer

ω scans

Absorption correction: numerical
(X-SHAPE and X-RED32; Stoe & Cie, 2008)

$T_{\min} = 0.837$, $T_{\max} = 0.966$

9692 measured reflections

3283 independent reflections

2634 reflections with $I > 2\sigma(I)$

$R_{\text{int}} = 0.041$

$\theta_{\max} = 27.0$ °, $\theta_{\min} = 2.1$ °

$h = -9 \rightarrow 9$

$k = -13 \rightarrow 13$

$l = -13 \rightarrow 13$

Refinement

Refinement on F^2

Least-squares matrix: full

$R[F^2 > 2\sigma(F^2)] = 0.046$

$wR(F^2) = 0.100$

$S = 1.06$

3283 reflections

188 parameters

0 restraints

Hydrogen site location: inferred from
neighbouring sites

H-atom parameters constrained

$w = 1/[\sigma^2(F_o^2) + (0.0383P)^2 + 0.2958P]$

where $P = (F_o^2 + 2F_c^2)/3$

$(\Delta/\sigma)_{\max} = 0.001$

$\Delta\rho_{\max} = 0.28$ e Å⁻³

$\Delta\rho_{\min} = -0.40$ e Å⁻³

Special details

Geometry. All esds (except the esd in the dihedral angle between two l.s. planes) are estimated using the full covariance matrix. The cell esds are taken into account individually in the estimation of esds in distances, angles and torsion angles; correlations between esds in cell parameters are only used when they are defined by crystal symmetry. An approximate (isotropic) treatment of cell esds is used for estimating esds involving l.s. planes.

Fractional atomic coordinates and isotropic or equivalent isotropic displacement parameters (\AA^2)

	<i>x</i>	<i>y</i>	<i>z</i>	$U_{\text{iso}}^*/U_{\text{eq}}$
Ni1	1.0000	0.5000	1.0000	0.04329 (15)
N1	1.1925 (3)	0.6472 (3)	0.9052 (2)	0.0544 (5)
C1	1.2695 (4)	0.7524 (3)	0.8535 (3)	0.0476 (6)
S1	1.38122 (12)	0.89701 (8)	0.77890 (9)	0.0675 (2)
N11	0.8623 (3)	0.5571 (2)	0.8151 (2)	0.0470 (5)
C11	0.9542 (4)	0.5796 (3)	0.6999 (3)	0.0511 (6)
H11	1.0844	0.5686	0.7029	0.061*
C12	0.8685 (4)	0.6177 (3)	0.5778 (3)	0.0516 (6)
H12	0.9387	0.6322	0.4987	0.062*
C13	0.6780 (4)	0.6350 (3)	0.5711 (3)	0.0476 (6)
C14	0.5829 (4)	0.6119 (3)	0.6894 (3)	0.0501 (6)
H14	0.4527	0.6230	0.6889	0.060*
C15	0.6789 (3)	0.5726 (3)	0.8082 (3)	0.0476 (6)
H15	0.6116	0.5558	0.8891	0.057*
C16	0.5863 (4)	0.6676 (3)	0.4381 (3)	0.0538 (6)
C17	0.4134 (4)	0.7550 (3)	0.4013 (3)	0.0553 (7)
C18	0.3648 (4)	0.8489 (3)	0.4564 (3)	0.0615 (7)
H18	0.4388	0.8554	0.5246	0.074*
C19	0.2080 (5)	0.9336 (4)	0.4122 (4)	0.0777 (10)
H19	0.1755	0.9989	0.4492	0.093*
C20	0.0997 (5)	0.9225 (4)	0.3144 (4)	0.0886 (12)
H20	-0.0074	0.9806	0.2840	0.106*
C21	0.1459 (5)	0.8281 (4)	0.2610 (4)	0.0868 (12)
H21	0.0694	0.8199	0.1949	0.104*
C22	0.3025 (5)	0.7452 (3)	0.3024 (3)	0.0700 (8)
H22	0.3350	0.6814	0.2637	0.084*
O11	0.6554 (3)	0.6210 (2)	0.3620 (2)	0.0687 (6)
N2	0.8453 (3)	0.6523 (2)	1.0367 (2)	0.0540 (6)
C2	0.7727 (4)	0.7466 (3)	1.0432 (3)	0.0518 (6)
C3	0.6820 (5)	0.8675 (3)	1.0510 (3)	0.0715 (9)
H3A	0.7191	0.9524	0.9733	0.107*
H3B	0.7171	0.8740	1.1348	0.107*
H3C	0.5484	0.8581	1.0501	0.107*

Atomic displacement parameters (\AA^2)

	U^{11}	U^{22}	U^{33}	U^{12}	U^{13}	U^{23}
Ni1	0.0442 (3)	0.0443 (3)	0.0446 (3)	0.00743 (19)	-0.00183 (19)	-0.0221 (2)
N1	0.0536 (13)	0.0556 (13)	0.0542 (14)	0.0029 (11)	-0.0014 (11)	-0.0230 (11)

C1	0.0488 (14)	0.0509 (15)	0.0481 (15)	0.0079 (12)	-0.0038 (12)	-0.0259 (12)
S1	0.0725 (5)	0.0514 (4)	0.0826 (6)	-0.0061 (4)	0.0032 (4)	-0.0317 (4)
N11	0.0465 (11)	0.0490 (12)	0.0479 (12)	0.0070 (9)	-0.0016 (9)	-0.0230 (10)
C11	0.0458 (13)	0.0620 (16)	0.0476 (15)	0.0031 (12)	0.0021 (11)	-0.0249 (13)
C12	0.0515 (14)	0.0575 (15)	0.0472 (15)	0.0018 (12)	0.0033 (12)	-0.0233 (12)
C13	0.0523 (14)	0.0456 (13)	0.0457 (14)	0.0028 (11)	-0.0034 (11)	-0.0199 (11)
C14	0.0475 (13)	0.0547 (15)	0.0508 (15)	0.0052 (11)	-0.0033 (12)	-0.0249 (12)
C15	0.0453 (13)	0.0539 (14)	0.0457 (14)	0.0072 (11)	-0.0006 (11)	-0.0234 (12)
C16	0.0590 (16)	0.0534 (15)	0.0479 (15)	-0.0010 (12)	-0.0051 (13)	-0.0197 (12)
C17	0.0565 (15)	0.0528 (15)	0.0472 (15)	-0.0032 (12)	-0.0049 (12)	-0.0110 (12)
C18	0.0587 (17)	0.0571 (16)	0.0586 (18)	0.0031 (13)	-0.0003 (14)	-0.0141 (14)
C19	0.069 (2)	0.066 (2)	0.080 (2)	0.0120 (16)	0.0040 (18)	-0.0139 (17)
C20	0.061 (2)	0.082 (2)	0.089 (3)	0.0105 (18)	-0.0111 (19)	-0.001 (2)
C21	0.068 (2)	0.089 (3)	0.076 (2)	-0.0072 (19)	-0.0239 (19)	-0.006 (2)
C22	0.074 (2)	0.0656 (19)	0.0601 (19)	-0.0066 (16)	-0.0159 (16)	-0.0149 (15)
O11	0.0799 (14)	0.0802 (14)	0.0541 (12)	0.0092 (11)	-0.0061 (11)	-0.0363 (11)
N2	0.0574 (13)	0.0568 (13)	0.0527 (13)	0.0123 (11)	-0.0055 (11)	-0.0282 (11)
C2	0.0606 (16)	0.0522 (15)	0.0468 (15)	0.0120 (13)	-0.0042 (12)	-0.0252 (12)
C3	0.093 (2)	0.0588 (17)	0.067 (2)	0.0288 (17)	-0.0073 (17)	-0.0328 (15)

Geometric parameters (Å, °)

Ni1—Ni ⁱ	2.038 (3)	C16—O11	1.217 (3)
Ni1—N1	2.038 (3)	C16—C17	1.494 (4)
Ni1—N2	2.093 (2)	C17—C18	1.383 (4)
Ni1—N2 ⁱ	2.093 (2)	C17—C22	1.395 (4)
Ni1—N11 ⁱ	2.108 (2)	C18—C19	1.390 (4)
Ni1—N11	2.108 (2)	C18—H18	0.9500
N1—C1	1.164 (3)	C19—C20	1.379 (5)
C1—S1	1.626 (3)	C19—H19	0.9500
N11—C15	1.339 (3)	C20—C21	1.371 (6)
N11—C11	1.343 (3)	C20—H20	0.9500
C11—C12	1.373 (4)	C21—C22	1.376 (5)
C11—H11	0.9500	C21—H21	0.9500
C12—C13	1.391 (4)	C22—H22	0.9500
C12—H12	0.9500	N2—C2	1.135 (3)
C13—C14	1.381 (4)	C2—C3	1.445 (4)
C13—C16	1.505 (4)	C3—H3A	0.9800
C14—C15	1.380 (4)	C3—H3B	0.9800
C14—H14	0.9500	C3—H3C	0.9800
C15—H15	0.9500		
N1 ⁱ —Ni1—N1	180.0	N11—C15—C14	123.2 (2)
N1 ⁱ —Ni1—N2	91.36 (9)	N11—C15—H15	118.4
N1—Ni1—N2	88.64 (9)	C14—C15—H15	118.4
N1 ⁱ —Ni1—N2 ⁱ	88.64 (9)	O11—C16—C17	121.0 (3)
N1—Ni1—N2 ⁱ	91.36 (9)	O11—C16—C13	118.7 (2)
N2—Ni1—N2 ⁱ	180.0	C17—C16—C13	120.3 (2)

N1 ⁱ —Ni1—N11 ⁱ	90.03 (9)	C18—C17—C22	119.4 (3)
N1—Ni1—N11 ⁱ	89.97 (9)	C18—C17—C16	122.7 (3)
N2—Ni1—N11 ⁱ	90.31 (8)	C22—C17—C16	117.9 (3)
N2 ⁱ —Ni1—N11 ⁱ	89.69 (8)	C17—C18—C19	120.1 (3)
N1 ⁱ —Ni1—N11	89.97 (9)	C17—C18—H18	120.0
N1—Ni1—N11	90.03 (9)	C19—C18—H18	120.0
N2—Ni1—N11	89.69 (8)	C20—C19—C18	119.8 (4)
N2 ⁱ —Ni1—N11	90.31 (8)	C20—C19—H19	120.1
N11 ⁱ —Ni1—N11	180.0	C18—C19—H19	120.1
C1—N1—Ni1	163.8 (2)	C21—C20—C19	120.3 (3)
N1—C1—S1	178.2 (2)	C21—C20—H20	119.9
C15—N11—C11	117.3 (2)	C19—C20—H20	119.9
C15—N11—Ni1	121.05 (18)	C20—C21—C22	120.5 (4)
C11—N11—Ni1	121.64 (17)	C20—C21—H21	119.8
N11—C11—C12	123.0 (2)	C22—C21—H21	119.8
N11—C11—H11	118.5	C21—C22—C17	120.0 (4)
C12—C11—H11	118.5	C21—C22—H22	120.0
C11—C12—C13	119.4 (3)	C17—C22—H22	120.0
C11—C12—H12	120.3	C2—N2—Ni1	171.5 (2)
C13—C12—H12	120.3	N2—C2—C3	179.4 (4)
C14—C13—C12	117.8 (2)	C2—C3—H3A	109.5
C14—C13—C16	123.6 (2)	C2—C3—H3B	109.5
C12—C13—C16	118.4 (2)	H3A—C3—H3B	109.5
C15—C14—C13	119.3 (2)	C2—C3—H3C	109.5
C15—C14—H14	120.4	H3A—C3—H3C	109.5
C13—C14—H14	120.4	H3B—C3—H3C	109.5

Symmetry code: (i) $-x+2, -y+1, -z+2$.

Hydrogen-bond geometry (\AA , $^\circ$)

<i>D</i> —H \cdots <i>A</i>	<i>D</i> —H	H \cdots <i>A</i>	<i>D</i> \cdots <i>A</i>	<i>D</i> —H \cdots <i>A</i>
C3—H3B \cdots S1 ⁱⁱ	0.98	2.98	3.662 (3)	127

Symmetry code: (ii) $-x+2, -y+2, -z+2$.